Communications in Transportation Research 4 (2024) 100133

Contents lists available at ScienceDirect

Communications in Transportation Research

journal homepage: www.journals.elsevier.com/communications-in-transportation-research

Full Length Article

Vehicle trajectory dataset from drone videos including off-ramp and congested traffic – Analysis of data quality, traffic flow, and accident risk

Moritz Berghaus [a,*], Serge Lamberty [a], Jörg Ehlers [a], Eszter Kalló [a], Markus Oeser [a,b]

[a] Institute of Highway Engineering, RWTH Aachen University, Aachen, 52074, Germany
[b] Federal Highway Research Institute, Bergisch Gladbach, 51427, Germany

ARTICLE INFO

Keywords:
Vehicle trajectory dataset
Traffic flow
Traffic safety
Computer vision

ABSTRACT

Vehicle trajectory data have become essential for many research fields, such as traffic flow, traffic safety, and automated driving. To make trajectory data useable for researchers, an overview of the included road section and traffic situation as well as a description of the data processing methodology is necessary. In this paper, we present a trajectory dataset from a German highway with two lanes per direction, an off-ramp and congested traffic in one direction, and an on-ramp in the other direction. The dataset contains 8,648 trajectories and covers 87 min and an ~1,200 m long section of the road. The trajectories were extracted from drone videos using a posttrained YOLOv5 object detection model and projected onto the road surface via three-dimensional (3D) camera calibration. The postprocessing methodology can compensate for most false detections and yield accurate speeds and accelerations. The trajectory data are also compared with induction loop data and vehicle-based smartphone sensor data to evaluate the plausibility and quality of the trajectory data. The deviations of the speeds and accelerations are estimated at 0.45 m/s and 0.3 m/s^2, respectively. We also present some applications of the data, including traffic flow analysis and accident risk analysis.

1. Introduction

Vehicle trajectory data or microscopic traffic data are highly valuable for a wide range of applications. The oldest application, starting with the famous Greenshields' study (Greenshields et al., 1935), was the analysis of traffic flow and the development and validation of traffic flow models. Treiterer (1975) was among the first researchers to collect vehicle trajectories using aerial images. The second application emerged in the 1980s with the Swedish Traffic Conflict Technique, which uses vehicle trajectories to evaluate traffic safety based on surrogate safety measures (SSMs), e.g., time to collision (TTC) (Hydén and Linderholm, 1984). While vehicle movements were analyzed manually in the beginning, image processing methods helped to automatically compute SSMs and identify traffic conflicts (Messelodi and Modena, 2005). The most recent application is the development of automated driving systems, which rely on naturalistic driving data to ensure that these systems interact safely with human drivers in every possible situation (Roesener et al., 2017). All these applications benefit from a wide variety of trajectory datasets with different road characteristics and traffic situations.

With the increasing number of applications, progress in computer vision technology has led to a growing number of trajectory datasets. The interest in publicly available datasets, such as the NGSIM dataset (U.S. Federal Highway Administration (FHWA), 2006), has shown that these datasets can be used for more than the application they were created for.

Most datasets contain only limited information on the data collection methodology and quality. Commonly used metrics in object detection, such as the mean average precision (mAP), represent only the quality of the position measurements, while most applications require velocity and acceleration. With appropriate postprocessing of the raw trajectory data, accurate velocities and accelerations can be achieved even with noisy position measurements. However, there is no standardized metric for evaluating the quality of processed trajectories. The trajectory dataset presented in this paper is compared with data from an induction loop and data from a smartphone sensor that was present in one of the vehicles included in the trajectory data. By comparing the speeds and accelerations, we can estimate the accuracy of the speed and acceleration values.

Although the purpose of publishing trajectory datasets is to make them useable for other researchers, it is often difficult for them to assess whether a dataset contains a suitable road section and suitable traffic scenarios for their research question. We therefore conduct a traffic flow analysis with time–space diagrams, fundamental diagrams, and time series of flow, density, and mean speed.

* Corresponding author.
E-mail address: berghaus@isac.rwth-aachen.de (M. Berghaus).

https://doi.org/10.1016/j.commtr.2024.100133
Received 26 January 2024; Received in revised form 9 April 2024; Accepted 9 April 2024

The trajectory dataset presented in this paper originates from a German highway with two lanes per direction, an off-ramp and congested traffic in one direction, and an on-ramp in the other direction. Based on the information on data quality, road characteristics, and traffic situations provided in this paper, researchers can evaluate whether the dataset meets their requirements.

The remainder of this paper is structured as follows. In Section 2, we provide an overview of other publicly available trajectory datasets. In Section 3, we present the data collection and data processing methodology. Section 4 contains the description of the data and an evaluation of the data quality. In Section 5, we present two possible applications of the dataset.

2. Related work

2.1. Vehicle trajectory datasets

When searching for comparable datasets, the high requirements in the area of traffic safety analysis and the complex boundary conditions that allow an evaluation of the infrastructure should not be neglected. The investigated datasets are compared and analyzed in this section.

The first category of datasets is generated from infrastructure-based sensors (Creß et al., 2022; U.S. FHWA, 2006; Wang et al., 2023). Here, the focus does not lie in the generation of particularly diverse data. Rather, with this kind of data generation, large amounts of data can be collected easily, e.g., for training vehicle behavior models. As the first large dataset of its kind, NGSIM (U.S. FHWA, 2006) demonstrated the possibility of microscopic traffic data collection by placing cameras on buildings, understandably with a small amount of data and noncomparable accuracy. The dataset presented in (Creß et al., 2022) comes from a large test site of the A9 highway in Germany, which covers a 3 km stretch of highway and is captured with lidar and cameras. A similar approach using radar was taken by Wang et al. (2023), where a dataset of several kilometers of highway in China was created. All three datasets and their corresponding methodologies show promising results but are too complex and expensive to perform on many different routes or have little lead time and low cost.

The remaining datasets used a similar approach as in this work: flying drones at a very high altitude either above or directly next to the highway. For example, Krajewski et al. (2018) acquired ~16.5 h of trajectory data from straight highway sections, and Moers et al. (2022) supplemented these data with on-ramp and off-ramp trajectories. The AUTOMATUM DATA dataset also provides a good basis for many applications with 30 h of material (Spannaus et al., 2021). The MAGIC dataset focuses on using a large number of drones simultaneously and uses a commercial service to extract the trajectories, which are detrimentally longer than those of any other dataset because of the large number of drones (Ma et al., 2022).

Although all of these works are very relevant and the data can be considered for many use cases, there is still room for improvement. These studies generally rely on a road surface consisting of a single flat area with no change in elevation. However, this approach works only when simple road geometries are used. The more complex the road infrastructure is, the larger the resulting errors will be. In contrast, this work uses three-dimensional (3D) models for the infrastructure, which allows these inaccuracies to be avoided.

2.2. Trajectory extraction methods

The generation of trajectory data has been a research topic for many years, such that a whole series of works is available. Various sensors and evaluation algorithms are used, often depending on the use case and users. For example, several laser scanners are fused for trajectory data (Zhao et al., 2009), and several lidar sensors (Kloeker et al., 2020) are used to capture trajectories at intersections. Furthermore, camera systems installed in the infrastructure can be used for recording trajectories. For example, in Clausse et al. (2019), a general framework with a method based on Mask R–CNN was presented for the extraction of 3D trajectories for the use of traffic cameras.

However, even when focusing on the acquisition of trajectories from drone videos, a multitude of works have attempted different methods with varying success. Azevedo et al. (2014) recognized the possibilities of a drone-based approach early on and extracted vehicle trajectories through background subtraction and a *k*-shortest disjoint path algorithm for tracking at a speed of two frames per second without classification. Apeltauer et al. (2015) used the AdaBoost classifier with multiblock local binary pattern (MB-LBP) for detection followed by the sequential Monte Carlo method to track vehicles through an intersection. Khan et al. (2017) used the Lucas–Kanade optical flow algorithm to detect and track vehicles in combination with background extraction. Zhao and Li (2019) used Mask R–CNN for detection combined with a semiautomatic extraction of different lanes but lacked a description of the method for camera calibration. Kim et al. (2019) compared the results from the aggregated channel feature (ACF) and Faster R–CNN methods for the tracking of vehicles in congested traffic situations and achieved promising results despite some problems with false positive detection. Ahmadi and Mohammadzadeh (2017) extracted vehicle trajectories from spaceborne videos using background subtraction with a much larger field of view but with no classification and a lower precision due to the lower resolution of the videos. Masouleh and Shah-Hosseini (2019) developed a new algorithm for the semantic segmentation of vehicles from UAV-based thermal infrared imagery using a Gaussian–Bernoulli restricted Boltzmann machine (GB-RBM) with improvements compared to other semantic segmentation networks. Feng et al. (2020) included pedestrians and cyclists in their YOLOv3-based approach and can therefore be used to record scenes on urban roads with all traffic participants, with an accuracy of approximately 92% for motor vehicles. Shi et al. (2021) used videos made from multiple helicopters to capture a larger section of a highway, and simultaneously, trajectory extraction with YOLOv3 automatically detected lane markings and calculated vehicle motion characteristics. Yeom and Nam (2021) approached the detection problem through the difference between two consecutive images for a driving vehicle and tracked the detected vehicles using a Kalman filter, sadly only using their method on a total of 22 vehicles in the recorded videos.

Furthermore, there are methods already listed in Section 2.1 that have already proven their potential with the publication of large datasets. As one of the first applications of neural networks for the extraction of vehicle trajectories from drone videos, Krajewski et al. (2018) used U-Net for the detection of vehicles and further started the extraction of parameters of interest for the automotive industry, such as maneuver classification. Using the same method, trajectories from intersections and exits were recorded in subsequent years (Krajewski et al., 2018; Moers et al., 2022).

Since the number of works on this topic is too large to cite them all in this work, the interested reader can refer to two reviews. In their review paper on drone-based road traffic monitoring systems, Bisio et al. (2022) presented additional approaches and datasets and compared different detection and tracking algorithms. Unfortunately, there is no mention of the different calibration methods used in the reviewed papers. Butilă and Boboc (2022) provide a systematic overview of 34 works on drone-based trajectory extraction, categorizing the works according to aim and feasibility.

3. Methods

In this section, we describe the workflow used to obtain the trajectory data presented in this paper. Section 3.1 contains all relevant information on the study area and the collection of the videos. Section 3.2 describes how the trajectories are extracted from the drone videos, including video stabilization, camera calibration, and vehicle detection. Section 3.3 contains the necessary steps of data processing to achieve a high-quality

trajectory dataset.

3.1. Study area and material collection

The dataset presented in this paper was collected at the highway A43 near Münster, Germany. The highway has two lanes in each direction, with a two-lane off-ramp in direction 1 (west to east) and a one-lane on-ramp in direction 2 (east to west). The dataset covers an ~1,200 m long stretch of road during the morning peak hour (7:11 to 8:38) on September 6, 2021. Direction 1 is partly congested during this time due to a nearby on-ramp. The data were collected at two locations using DJI Mavic Pro drones. Two drones per location were used alternately due to limited battery capacity. As a result, there are some temporal overlaps and gaps in the videos, which must be considered during data processing. The drones flew 500 m above ground and each covered more than 600 m of the road with a spatial overlap of ~50 m. The videos were recorded with 4 K resolution (3,840 × 2,160) at 25 frames per second, which corresponds to a vehicle size of approximately 30 × 12 pixels. Fig. 1 shows two aerial views of the filmed road section.

To check the plausibility of the vehicle trajectories derived from drone data, additional measurements were taken with a vehicle that was traveling on the highway section during the time of video recording. A smartphone's GPS sensor and inertial measurement unit captured the vehicle's position, speed, and acceleration at frequencies of 1 Hz (position and speed) and 100 Hz (acceleration), respectively. The smartphone was mounted on a flat surface approximately at the center of the vehicle to ensure that it remained aligned in the vehicle coordinate system at all times. The data were collected with an iPhone X and the app PhyPhox, which allows the recording of raw sensor data (Staacks et al., 2018). To ensure that the vehicle was easily visible in the video images, an orange van (VW Transporter) was used. This ensures that the drone data can be correctly assigned to this vehicle and that the drone and vehicle data can be compared correctly.

3.2. Trajectory extraction

3.2.1. Stabilization

The first step in evaluating drone images is usually video stabilization. Since the calibration step explained in the next section can only be performed on the first frame of each video, each subsequent frame in the video is transformed to match this first frame. The stabilization is performed based on a standard pipeline using feature detection from Shi and Tomasi (1994), the Lucas–Kanade feature tracking method presented in Bouguet (1999), and the computation of a homography via RANSAC. If the computation of the homography is successful, the current image can be deformed accordingly. In the case of particularly abrupt movements of the drone or continuous displacement of the image and thus too large a deviation, stabilization is interrupted, and the video is split, removing up to 2 s of video to eliminate any blurred images. Editing of the video is initiated in the event that less than 5% of the features found can be recovered by homography.

3.2.2. Calibration

Calibration of the video corresponds to the process of finding a transformation matrix for converting two-dimensional (2D) image coordinates to 3D world coordinates. The intrinsic camera parameters (focal length and distortion) of the drone were computed in preparation for the evaluation and used for the extrinsic calibration process.

For the extrinsic calibration, the first step is to create a 3D model of the road markings using publicly available geodata (georeferenced orthophotos and an elevation model from laser scanner data) from North Rhine–Westphalia (GDI NRW, 2024) (Fig. 2). Since the resulting model does not show a single straight road surface as in other works but rather a more realistic 3D surface, it is approximated with triangulation. Instead of calculating a single transformation for the entire road surface, as is usually the case; in our case, each triangulation surface receives a separate transformation. With the 3D model, reference points can be captured, and the different transformations can be computed in a final step.

3.2.3. Detection and tracking

The detection of vehicles in single frames is performed with a post-trained model based on YOLOv5 (Jocher et al., 2022). For this purpose, several minutes of video footage were labeled by hand and used via transfer learning to adapt an existing model. The trained model provides excellent results in detecting vehicles (mAP@0.5 of 95%). A slight tendency toward false-positive results can be remedied in the future via further training; in our case, false detections are reliably eliminated by tracking and postprocessing of the trajectories. Accordingly, in the present work, not single detections are a criterion of the data quality but rather the complete trajectories (see Section 4). These trajectories are created in the first step by matching the positions and the driving direction. In all further steps, the distance between two detections is no longer determined, but the distance between the current position and the position is predicted on the basis of the speed recorded thus far. Munkres (1957) is used as the matching algorithm. Even if a vehicle is covered by a bridge or gantry for a short period, this algorithm can track it in most cases. Fig. 3 shows a snapshot of a drone video with the vehicle detections reprojected into the image.

3.3. Data processing

Data processing ensures that the vehicle trajectories are plausible and that the trajectories extracted from each video are combined into a single dataset.

The first step is to convert the vehicle positions from world coordinates to road coordinates, i.e., a coordinate system where the x-axis lies on the right edge of the rightmost lane and the y-axis is orthogonal to the x-axis. Thus, the x value represents the distance traveled by a vehicle, and the y value represents the distance to the right edge of the road, which can be used to determine the lane on which the vehicle drives. This coordinate system is convenient for most applications involving inter-urban roads, where all vehicles drive in the same direction, and mostly only the velocities and accelerations in the driving direction are relevant. The road markings were extracted as polygonal chains from georeferenced orthophotos (see Section 3.2) and then smoothed.

The road coordinates are also useful for checking the plausibility of the data. It can be assumed that vehicles only drive forward, i.e., the velocity in the x-direction must not be smaller than zero. It can also be assumed that the velocity has an upper bound. Therefore, the difference between two subsequent x values (Δx) is a criterion for plausibility. The

Fig. 1. Aerial views of the filmed road section. (a) Western region and (b) eastern region.

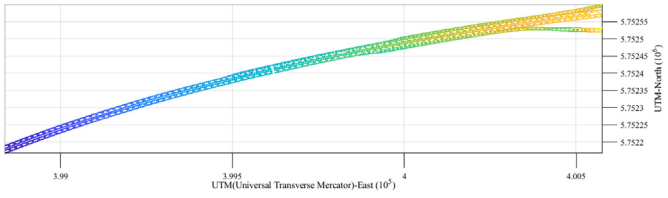

Fig. 2. 3D-street model of the recorded highway segment, color-coded according to the z-axis.

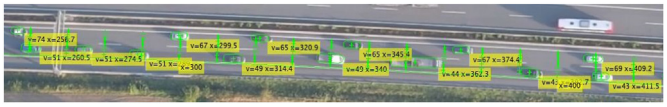

Fig. 3. Snapshot of a drone video with vehicle detections.

difference between two subsequent y values should be limited more strictly because lateral velocities are usually much smaller than longitudinal velocities. A large time gap between two subsequent data points of the same vehicle is another criterion that has also proven to be a criterion for implausibility. The implausible points are removed from the data to remove all single outliers. The plausibility is checked again with the remaining data points. This procedure is applied until multiple subsequent outliers are removed. To identify data points of a trajectory that do not belong to the same vehicle, the trajectory is split if implausible points remain after several iterations. In this case, a new vehicle ID is assigned to one part of the trajectory. Fig. 4 shows that most obvious errors in the data can be removed by this method. Most of these errors result from vehicle tracks that are matched to a nonmoving false positive detection, e.g., the shadow of a tree.

To obtain realistic velocities and accelerations, the trajectories are then smoothed by fitting a smoothing spline to the data. The smoothing parameter must be selected depending on the magnitude of the outliers that have not been removed during the plausibility check. In our dataset, smoothing parameters of 0.2 in the x-direction and 0.5 in the y-direction were shown to be suitable. Fig. 5 shows that this process can successfully remove the outliers.

Next, the trajectories extracted from different videos are combined. Since the timestamps of the videos are not perfectly synchronized, the trajectories must be shifted temporally by a few seconds. Since the number of videos is not too high, this step can be performed manually. The trajectories of two adjacent (spatially or temporally) videos are plotted with different shift values, and the best fit is selected (Fig. 6).

Many vehicles are represented in the raw data by more than one trajectory either because they are not tracked correctly (Fig. 4) or because they appear in more than one video (Fig. 6). Therefore, overlapping or adjacent trajectories that belong to the same vehicle must be identified and joined. If the distance in the x-direction is smaller than 5 m and the distance in the y-direction is smaller than 2.5 m, the trajectories are considered to overlap. In this case, one of the trajectories is removed. If the last point of one trajectory and the first point of another trajectory are closer than 10 m in the x-direction and 3 m in the y-direction, they are joined because they likely belong to the same vehicle (Fig. 7). With this method, vehicles can be tracked even in situations where the Kuhn–Munkres algorithm fails. The joined trajectories are then smoothed again. Short trajectories (< 3 s) are removed from the dataset because they are likely false positive detections, as mentioned above.

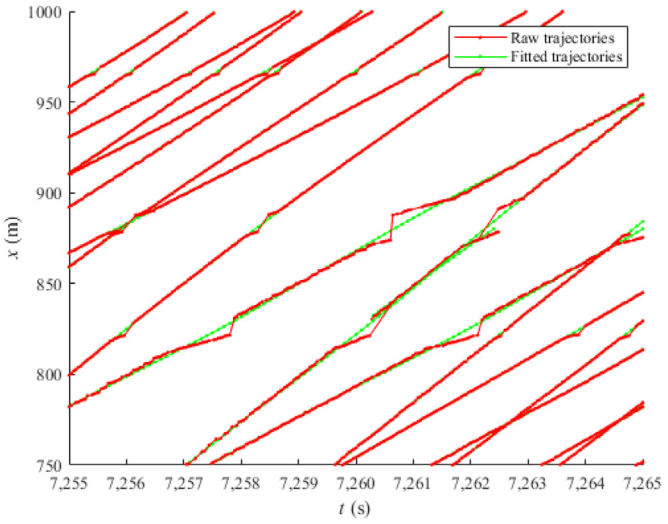

Fig. 5. Comparison of raw trajectories (after removing implausible points) and fitted trajectories.

4. Description and evaluation of the dataset

The dataset contains 5,016 trajectories in direction 1 and 3,632 trajectories in direction 2. Regarding the sensitivity of the recorded data, a random sample analysis of approximately 450 vehicles showed that only approximately 0.45% of the vehicles actually present were not detected. These vehicles are gray; hence, their contrast to the road pavement is very small. False detections could not be identified in the sample, mainly due to trajectory postprocessing, which removes any trajectories that are too short. In direction 1, 3,993 trajectories (79.5%) are longer than 90% of the length of the filmed road section (direction 2: 2,928 trajectories, 80.6%). The remaining vehicles are represented in the dataset by two or more shorter trajectories with small gaps that cannot be filled by the data processing methodology. These shorter trajectories can still be used for traffic flow and accident risk analyses.

We provide the data in two different formats: for MATLAB users in.mat format and for all other users in.csv format.

In .mat format, the data are provided in a cell array where each cell contains the data of a single vehicle. The data of a single vehicle are organized in a structure array ("struct"). The struct contains time-dependent and time-independent data. The time-independent data include the vehicle ID, a description of the vehicle category (passenger car, bus, truck, etc.), a corresponding ID of the vehicle category, the vehicle length and width in (m), and the 2D contour (n-by-2 table, where $X = 0$ and $Y = 0$ are the vehicle centroid). The time-dependent data include the trajectory. The original (unprocessed) trajectory is an n-by-6 table with a vehicle ID, 2D positions in the road coordinate system in (m)

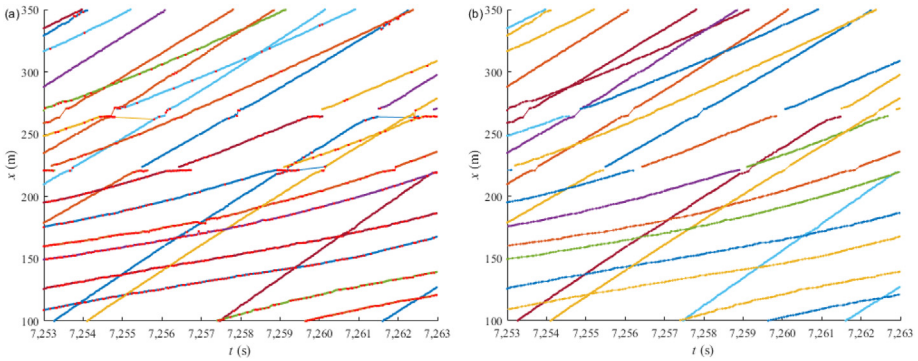

Fig. 4. (a) Raw data with implausible points marked in red. (b) Data after removal of implausible points.

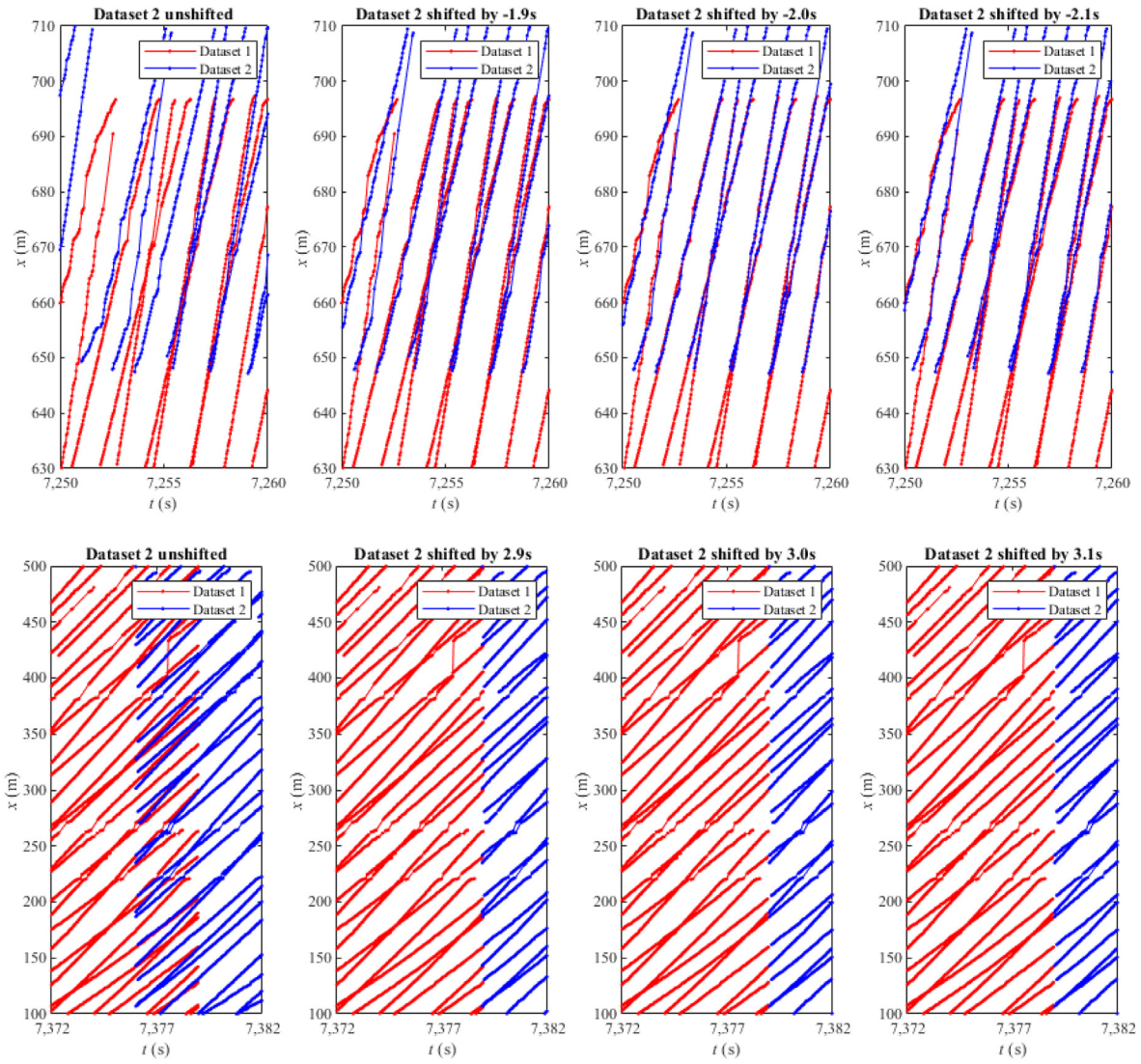

Fig. 6. Identifying the shift between two adjacent (temporal or spatial) videos.

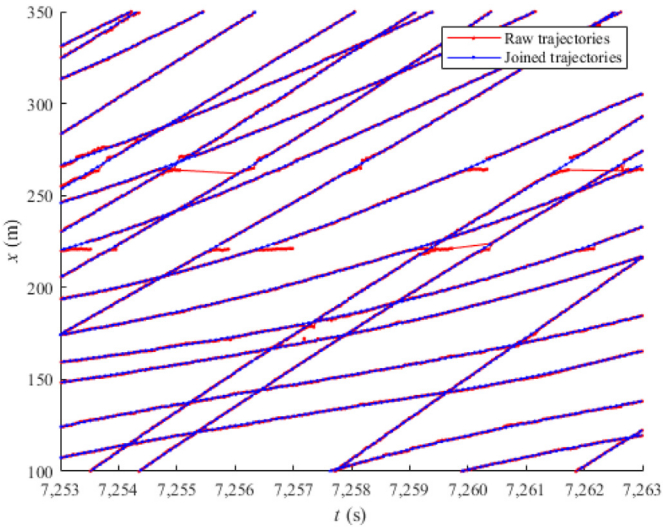

Fig. 7. Raw data (red) and trajectories after all data processing steps (blue).

(x is the direction along the road, y is orthogonal to x), a timestamp in (s) (starting at September 6, 2021, 6 a.m.), and 2D positions in the global UTM coordinate system. The fitted (processed) trajectory is an n-by-3 table with 2D positions in the road coordinate system and timestamps, an n-by-3 table with 2D speeds in the road coordinate system and timestamps, and an n-by-3 table with 2D accelerations in the road coordinate system and timestamps.

For MATLAB users, we also provide a small toolbox that enables some basic analyses and visualizations.

In the .csv format, the data are provided in a table with the following columns: timestamp in (s) (starting at September 6, 2021, 6 a.m.), timestamp in "yyyy-MM-dd HH:mm:ss.s", vehicle ID, a description of the vehicle category (passenger car, bus, truck, etc.), vehicle length and width in (m), and the fitted (processed) trajectory with the 2D-positions in (m), 2D-speeds in (m/s) and 2D-accelerations in (m/s^2) in the road coordinate system in (m) (x is the direction along the road, y is orthogonal to x).

The dataset and the MATLAB toolbox can be downloaded at https://data.isac.rwth-aachen.de (Berghaus et al., 2022).

4.1. Macroscopic comparison with induction loop data

Using data from nearby induction loops provided by the road operator Die Autobahn GmbH des Bundes (Mobilithek, 2022), the flow and mean speeds computed with our dataset can be compared to the flow and mean speeds measured by the induction loops. First, we use data from

two induction loops (one on each lane, only direction 1) that are located in the middle of the filmed road section. Fig. 8 shows that both the flows and the mean speeds from the drone dataset are consistent with the flows and mean speeds from the induction loop data. However, the flows from the drone dataset are mostly slightly smaller, which indicates that not all vehicles have been detected. The root mean square (RMS) deviation of the flows is 2.2 vehicles per minute in lane 1 and 3.1 vehicles per minute in lane 2. The speeds from the drone data are also generally slightly lower. The RMS deviation of the speeds is 0.78 m/s (2.8 km/h) in both lanes. Since the accuracy of the speed measurement of the induction loops is unknown, it cannot be concluded which values are more accurate.

The data from the adjacent induction loops can be used to interpolate the mean speeds in the filmed road section. Due to the propagation of shock waves (forward in free flow conditions and backward in congested flow conditions), linear interpolation is not appropriate. Instead, we use the adaptive smoothing method (ASM) proposed by Treiber and Helbing (2002), which takes the propagation of shock waves into account. Fig. 9 shows good agreement between the mean speeds obtained from the trajectory data and the interpolated mean speeds obtained from the induction loop data.

The induction loops categorize the vehicle flows into passenger cars and trucks. In direction 1, the truck ratio is 8.2% (direction 2: 10.5%) according to the induction loop data and 12.3% (direction 2: 11.5%) according to the trajectory data. These differences indicate that some passenger cars might have been falsely labeled as trucks in the trajectory data. However, the accuracy of vehicle categorization in induction loop data cannot be validated.

4.2. Microscopic comparison with in-vehicle sensors

To check the plausibility of the calculated speeds and accelerations obtained from drone data, eight test runs with in-vehicle sensors were performed, four in each direction. Similar to the drone data, in-vehicle data were smoothed to reduce signal noise. A smoothing spline with break points of 0.5 s for the accelerometer and 2 s for the GPS was used. These parameters were chosen to filter out sensor noise without compromising the validity of the data. For a valid comparison between drone data and in-vehicle data, the clocks of both data sources were aligned based on the position data. The signals of the in-vehicle sensors were shifted by the time difference between the drone and in-vehicle sensor data at the position where the measurement vehicle was first detected by the drone.

Fig. 10 shows good agreement between the speeds derived from drone data and the speeds obtained from in-vehicle sensors. The deviations between the signals of the two data sources are normally distributed, with a mean of 0.01 m/s and a standard deviation of 0.47 m/s. Thus, no systematic deviation can be identified. The mean correlations between the signals are 0.99 (direction 1) and 0.90 (direction 2). The RMS deviations between the signals are on average 0.43 m/s (direction 1) and 0.46 m/s (direction 2).

The travel direction (x-direction) and direction orthogonal to the travel direction (y-direction) of acceleration are compared. The general patterns of the drone data and in-vehicle sensor data are similar in both x-direction (Fig. 11) and y-direction (Fig. 12), which is also indicated by low average RMS deviations (Table 1). However, high-frequency changes in acceleration cannot be detected in the drone data. This is particularly noticeable in y-direction. Lane changes are clearly recognizable as peaks with in-vehicle data, while the signal derived from drone data is substantially smoothed. This is also reflected in a low correlation in y-direction between the two data sources. In addition, there is an offset in x- and y-directions, which changes between runs. This could be due to small movements of the smartphone mount between runs, as the offset is constant during each test run.

Compared to the speed differences between induction loops and drone data, the differences between in-vehicle data and drone data are substantially smaller. This indicates that the induction loops on this section of the road might not be well calibrated for speed measurements. Therefore, the comparison with the in-vehicle data confirms the high quality of the drone data.

5. Possible applications of the dataset

5.1. Traffic flow analysis

In the following, we present a microscopic and macroscopic traffic flow analysis based on trajectory data. Fig. 13 shows two time–space diagrams of an excerpt of the data. The color-coding of the lanes (Fig. 13a) illustrates the frequency and locations of lane changes, the gaps between vehicles and the speed differences between the lanes. The color coding of the speed (Fig. 13b) illustrates the propagation of shock waves.

The time series of flow, density, and mean speed in 1-min interval (Fig. 14) allow the identification of congestion and the distribution of vehicles between lanes. There are two stop-and-go waves (7:46 and 7:53) with large densities and low speeds in both lanes. Due to the small length of these stop-and-go waves, the flow does not decrease significantly. As expected, the mean speed in lane 2 is greater than that in lane 1 due to the presence of fewer trucks in lane 1.

The flow–density diagram, speed–flow diagram, and speed–density diagram (Fig. 15) show the capacity, optimal speed, and critical density on this road section, respectively. Again, the small length of the stop-and-go waves leads to densities up to 57 veh/km per lane, which is well below the maximum jam density.

5.2. Accident risk analysis

The concept of traffic conflict analysis is based on the assumption that

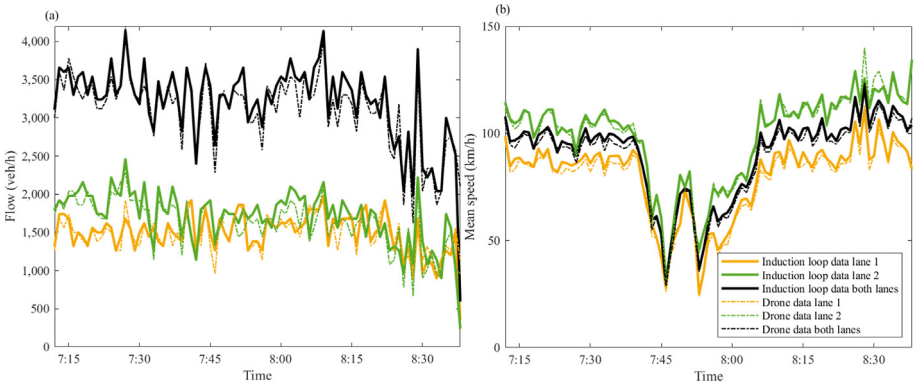

Fig. 8. Comparison of induction loop data and drone data with respect to (a) flow and (b) mean speed in 1-min-intervals.

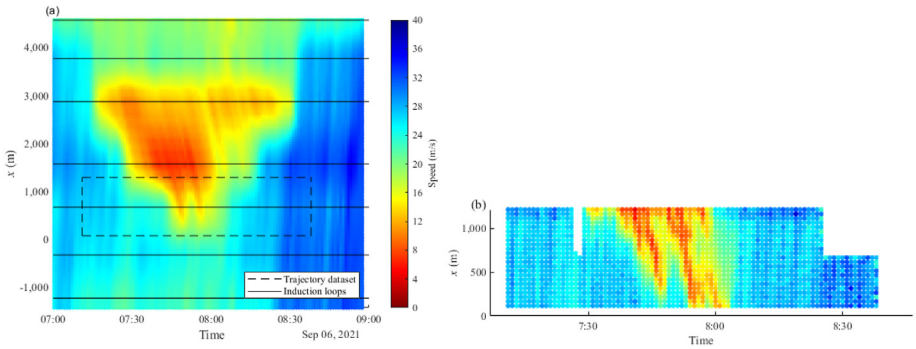

Fig. 9. Comparison of (a) mean speeds obtained from induction loop data and the adaptive smoothing method and (b) the mean speeds obtained from our trajectory data.

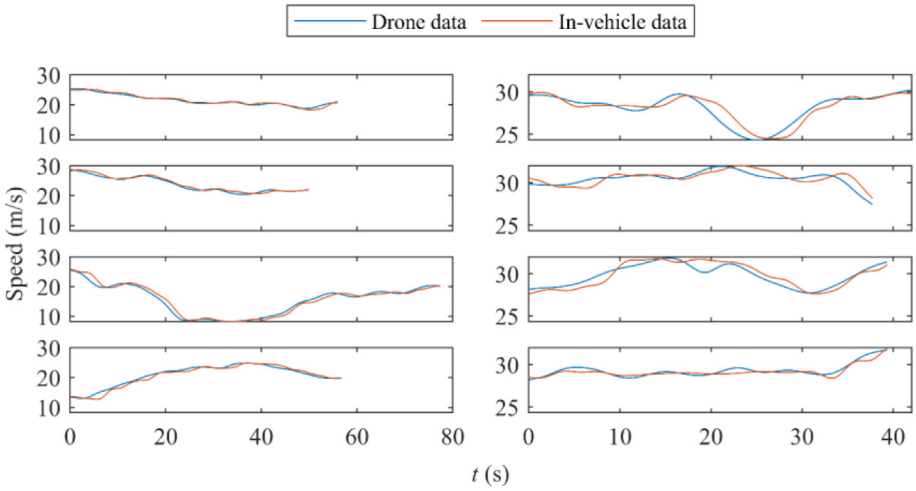

Fig. 10. Comparison of the speeds of the measurement vehicle obtained from drone data (blue lines) and from in-vehicle data (orange lines) of eight test runs (left: direction 1, right: direction 2).

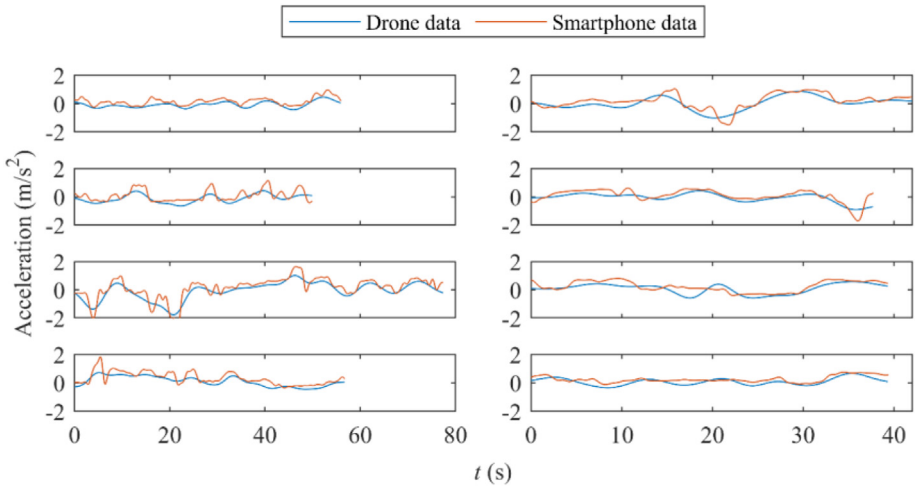

Fig. 11. Comparison of the accelerations along the road (*x*-direction) of the measurement vehicle obtained from drone data (blue lines) and from in-vehicle data (orange lines) from eight test runs (left: direction 1, right: direction 2).

each traffic interaction can lead to a collision. The less likely the participants of a traffic interaction are to react and avoid a crash, the more dangerous the situation is evaluated. To determine this "closeness" to a crash, different surrogate safety measures (SSMs) have been developed in recent decades. According to Mahmud (Mahmud et al., 2017), these SSMs can be categorized as follows: (1) temporal-proximal indicators, (2) deceleration-based indicators, and (3) distance-based proximal indicators.

In the first two categories, time-to-collision (TTC) and deceleration rate to avoid crash (DRAC) are two of the most commonly used measures

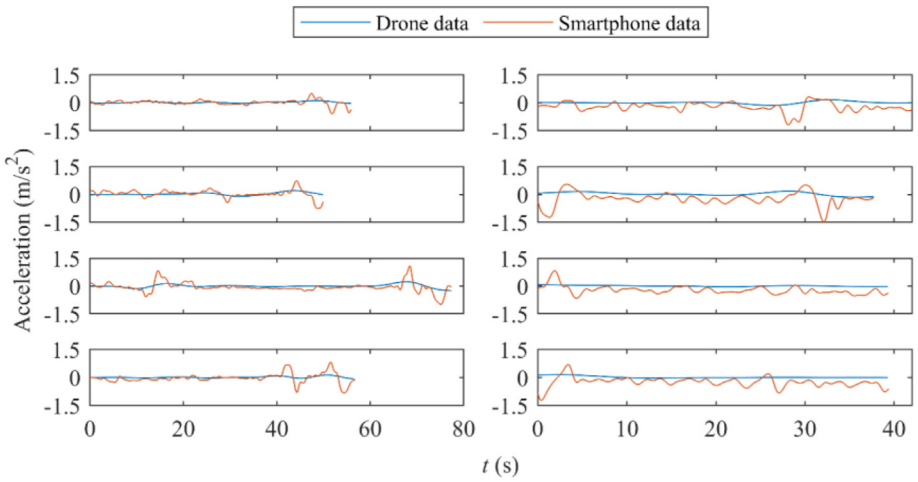

Fig. 12. Comparison of the accelerations orthogonal to the road (*y*-direction) of the measurement vehicle obtained from drone data (blue lines) and from in-vehicle data (orange lines) from eight test runs (left: direction 1, right: direction 2).

Table 1
Parameters for comparing acceleration data derived from drone data and acceleration data obtained from the in-vehicle sensor.

Signal		Mean of deviations (m/s^2)	Std.–Dev. (m/s^2)	Correlation	Average RMS deviations (m/s^2)
Acceleration in *X*	Direction 1	0.23	0.25	0.83	0.33
	Direction 2	0.16	0.23	0.80	0.28
Acceleration in *Y*	Direction 1	−0.03	0.20	0.45	0.20
	Direction 2	−0.24	0.26	0.36	0.26

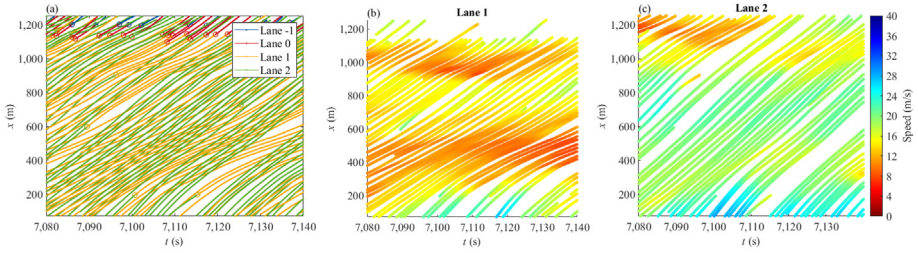

Fig. 13. Time–space diagrams with (a) color-coded lanes and speeds in lanes (b) 1 and (c) 2.

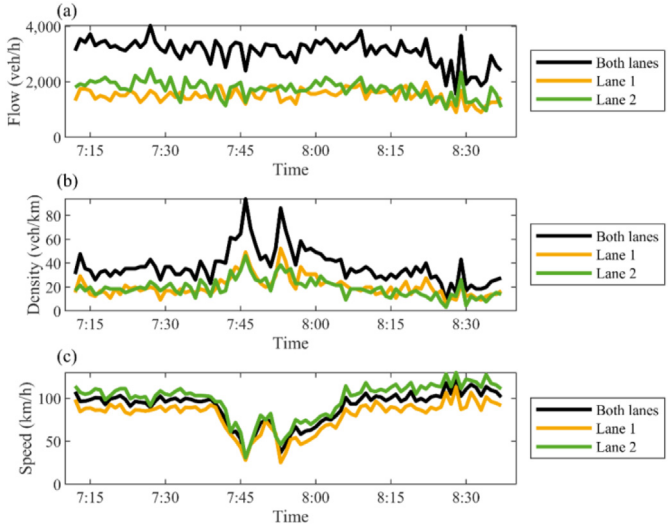

Fig. 14. Time series of (a) flow, (b) density, and (c) mean speed.

to analyze traffic safety. Both of these SSMs rely on the assumptions that the analyzed traffic participants will maintain their course and momentum from the initial moment until a collision occurs. In this way, the TTC determines the remaining time until the collision from this initial moment, whereas the DRAC estimates the smallest deceleration rate needed to avoid the collision (Almqvist et al., 1991; Hayward, 1971).

However, both in inner-city traffic and on highways, acceleration and deceleration of the traffic participants cannot be neglected. Therefore, to evaluate the traffic on the recorded road section, we applied modified versions of these two indicators: We used the modified time-to-collision (MTTC) and deceleration rate to avoid crashes using constant initial acceleration (DCIA). The MTTC was developed by Ozbay et al. (2008) and can be calculated as Eq. (1):

$$\mathrm{MTTC} = \begin{cases} \dfrac{D}{v_\mathrm{d}}, \text{if } v_\mathrm{d} > 0 \text{ and } a_\mathrm{d} = 0 \\ \dfrac{-v_\mathrm{d} \pm \sqrt{v_\mathrm{d}^2 + 2a_\mathrm{d}D}}{a_\mathrm{d}}, \text{if } a_\mathrm{d} \neq 0 \end{cases} \tag{1}$$

where $v_\mathrm{d} = v_\mathrm{F} - v_\mathrm{L}$ is the initial speed difference between the speed of the follower v_F and the speed of the leader v_L vehicles, $a_\mathrm{d} = a_\mathrm{F} - a_\mathrm{L}$ is the acceleration difference, and D is the initial net distance between the

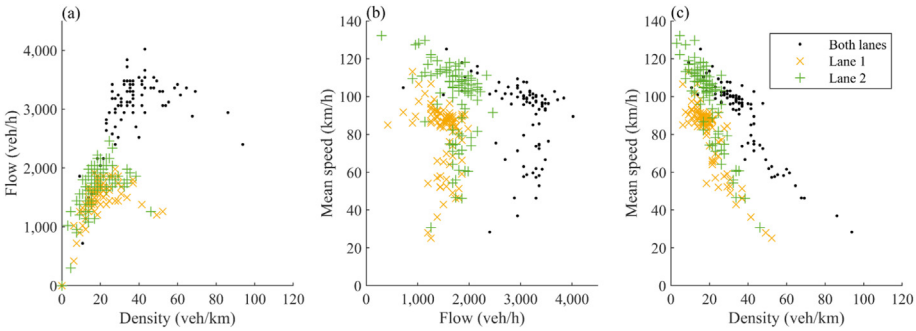

Fig. 15. (a) Flow–density diagram, (b) speed–flow diagram, and (c) speed–density diagram.

vehicles. MTTC is the smallest positive result. When the MTTC is equal to or lower than 1.5 s, the interaction is considered risky (Ozbay et al., 2008).

The DCIA was developed by Fazekas et al. (2017) and can be calculated as Eq. (2):

$$\mathrm{DCIA} = \frac{d_L T + v_L - d_F R - v_F}{T - R}, \text{if } T > R \tag{2}$$

where v_F, v_L, d_F, and d_L are the initial speed and initial deceleration of the follower and leader vehicles, respectively. R is the reaction time of the follower vehicle. T is the time until a crash, which can be calculated as Eq. (3):

$$T = \frac{v_F R - v_L R - 2D}{v_L + d_L R - v_F - d_F R}, \text{if denom.} \neq 0 \tag{3}$$

when the DCIA is above 3.4 m/s^2, the interaction is considered dangerous (Fazekas et al., 2017).

Due to the traffic data collection method described above, SSMs can be calculated at any timestamp in this dataset. This allows us to determine the extreme values of TTC and DCIA between interacting vehicles, which enables the analysis of the whole traffic scene. For this purpose, we built so-called pairs of interacting vehicles (one follower and one leader vehicle) that could collide based on their momentum. In the case of MTTC, we then determined the lowest value of each vehicle pair, whereas for DCIA, we identified the highest deceleration rates between the paired vehicles. In the next step, we located these extreme values on the positions of the follower vehicles on the road. Then, we calculated the average value of these results in each 20 m long section on the analyzed road section for each traffic lane separately. To present only relevant information, we considered only MTTC values under 5 s. Accordingly, Fig. 16 shows the average MTTC, and Fig. 17 shows the average DCIA values in the west-to-east travel direction. The values are presented with colors: The riskier the interaction based on the SSM is, the darker the red is.

The average MTTC values were less than the threshold value of 1.5 s in the main lane (lane 1) in 23% of the 20 m long road sections, in the passing lane (lane 2) in 27.9% and in the first exit lane (lane 0) in 18.2%. In contrast to the MTTC, the average DCIA values did not reach the

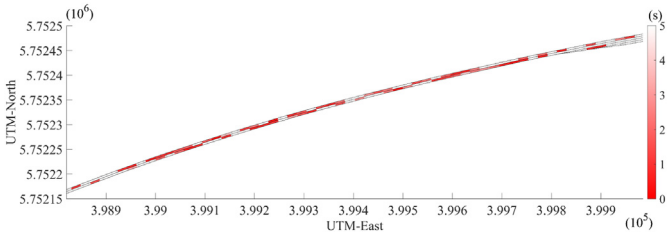

Fig. 16. Average MTTC values under 5 s in 20 m long sections from the west to the east.

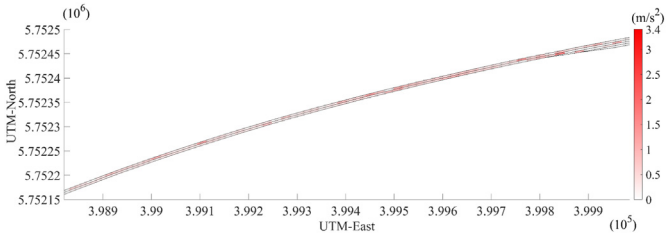

Fig. 17. Average DCIA values in 20 m long sections from the west to the east.

threshold value of 3.4 m/s^2 on the road section. In fact, the highest average value present in the data was 1.69 m/s^2, which, although corresponding to stronger braking, still falls within the range of normal occurrences in traffic. The results can be explained by the congested traffic, where vehicles are relatively close to each other; therefore, the time to a crash is low, while due to lower speed values, traffic participants do not need to brake strongly to avoid a collision.

6. Conclusions

This study presented a vehicle trajectory dataset from a German highway with two lanes and an off-ramp as well as the methods implemented to create the dataset. The data contain both free and congested traffic. The data extraction and processing methodology is applicable to other drone videos and, to some extent, to videos from stationary cameras. We performed a traffic flow analysis and an accident risk analysis, which showed that the trajectory data are suitable for these two applications. We also evaluated the plausibility and quality of the data by comparing the speeds, accelerations and flows with the results from induction loop data and smartphone accelerometer data. The results showed good agreement between our dataset and the other sensor data, which indicates good data quality. We therefore conclude that the dataset is useable for traffic flow and traffic safety analyses.

Replication and data sharing

The data presented in the manuscript can be accessed at https://data.isac.rwth-aachen.de/?p=58.

CRediT authorship contribution statement

Moritz Berghaus: Writing – review & editing, Writing – original draft, Visualization, Validation, Methodology, Investigation, Formal analysis, Data curation, Conceptualization. **Serge Lamberty:** Writing – review & editing, Writing – original draft, Software, Methodology, Formal analysis, Data curation, Conceptualization. **Jörg Ehlers:** Writing – review & editing, Writing – original draft, Visualization, Validation, Methodology, Investigation, Formal analysis, Data curation, Conceptualization. **Eszter Kalló:** Writing – review & editing, Writing – original

draft, Visualization, Methodology, Formal analysis, Conceptualization. **Markus Oeser:** Supervision, Project administration, Funding acquisition.

Declaration of competing interest

The authors declare th at they have no known competing financial interests or personal relationships that could have appeared to influence the work reported in this paper.

Acknowledgements

The work presented in this study is part of the projects BueLaMo (Bürgerlabor Mobiles Münsterland - Citizens' Laboratory Mobile Münsterland) funded by the German Federal Ministry for Education and Research, FeGis+ (Früherkennung von Gefahrenstellen im Straβenverkehr - Early Detection of Dangerous Areas in Traffic) funded by the German Federal Ministry for Digital and Transport, and NeMo (Neue Ansätze der Verkehrsmodellierung unter Berücksichtigung komplexer Geometrien und Daten - New traffic models considering complex geometries and data) funded by the German Research Foundation (DFG).

References

Ahmadi, S.A., Mohammadzadeh, A., 2017. A simple method for detecting and tracking vehicles and vessels from high resolution spaceborne videos. In: 2017 Joint Urban Remote Sensing Event (JURSE), pp. 1–4.
Almqvist, S., Hyden, C., Risser, R., 1991. Use of speed limiters in cars for increased safety and a better environment. Transport. Res. Rec. 34–39.
Apeltauer, J., Babinec, A., Herman, D., Apeltauer, T., 2015. Automatic vehicle trajectory extraction for traffic analysis from aerial video data. Int. Arch. Photogram. Rem. Sens. Spatial Inf. Sci. 40, 9–15.
Azevedo, C.L., Cardoso, J.L., Ben-Akiva, M., Costeira, J.P., Marques, M., 2014. Automatic vehicle trajectory extraction by aerial remote sensing. Procedia Soc. Behav. Sci. 111, 849–858.
Berghaus, M., Lamberty, S., Ehlers, J., Kallo, E., Oeser, M., 2022. Vehicle trajectory dataset from drone videos including off-ramp and congested traffic. https://data.isac.rwth-aachen.de.
Bisio, I., Garibotto, C., Haleem, H., Lavagetto, F., Sciarrone, A., 2022. A systematic review of drone based road traffic monitoring system. IEEE Access 10, 101537–101555.
Bouguet, J., 1999. Pyramidal Implementation of the Lucas Kanade Feature Tracker, vol. 16. Intel Corp., Microprocessor Research Labs, Santa Clara, CA.
Butilă, E.V., Boboc, R.G., 2022. Urban traffic monitoring and analysis using unmanned aerial vehicles (UAVs): a systematic literature review. Rem. Sens. 14, 620.
Clausse, A., Benslimane, S., de La Fortelle, A., 2019. Large-Scale extraction of accurate vehicle trajectories for driving behavior learning. In: 2019 IEEE Intelligent Vehicles Symposium (IV), pp. 2391–2396.
Creß, C., Zimmer, W., Strand, L., Fortkord, M., Dai, S., Lakshminarasimhan, V., et al., 2022. A9-dataset: multi-sensor infrastructure-based dataset for mobility research. In: 2022 IEEE Intelligent Vehicles Symposium (IV), pp. 965–970.
Fazekas, A., Hennecke, F., Kalló, E., Oeser, M., 2017. A novel surrogate safety indicator based on constant initial acceleration and reaction time assumption. J. Adv. Transport. 2017, 8376572.
Feng, R., Fan, C., Li, Z., Chen, X., 2020. Mixed road user trajectory extraction from moving aerial videos based on convolution neural network detection. IEEE Access 8, 43508–43519.
GDI NRW, 2024. Geoportal.NRW. https://www.geoportal.nrw.
Greenshields, B., Bibbins, J., Miller, H., 1935. A study of traffic capacity. In: https://onlinepubs.trb.org/Onlinepubs/hrbproceedings/14/14P1-023.pdf.
Hayward, J.C., 1971. Near Misses as a Measure of Safety at Urban Intersections. M.S. Thesis. The Pennsylvania State University, Philadelphia, PA, USA.
Hydén, C., Linderholm, L., 1984. The Swedish traffic-conflicts technique. In: Asmussen, E. (Ed.), International Calibration Study of Traffic Conflict Techniques, pp. 133–139.
Jocher, G., Chaurasia, A., Stoken, A., Borovec, J., Kwon, Y., Fang, J., et al., 2022. Ultralytics/yolov5: v6. 1-tensorrt, tensorflow edge tpu and openvino export and inference. https://github.com/ultralytics/yolov5/discussions/6740.
Khan, M.A., Ectors, W., Bellemans, T., Janssens, D., Wets, G., 2017. Unmanned aerial vehicle–based traffic analysis: methodological framework for automated multivehicle trajectory extraction. Transport. Res. Rec. 2626, 25–33.
Kim, E.J., Park, H.C., Ham, S.W., Kho, S.Y., Kim, D.K., 2019. Extracting vehicle trajectories using unmanned aerial vehicles in congested traffic conditions. J. Adv. Transport. 2019, 9060797.
Kloeker, L., Geller, C., Kloeker, A., Eckstein, L., 2020. High-precision digital traffic recording with multi-LiDAR infrastructure sensor setups. In: 2020 IEEE 23rd International Conference on Intelligent Transportation Systems (ITSC), pp. 1–8.
Krajewski, R., Bock, J., Kloeker, L., Eckstein, L., 2018. The highD dataset: a drone dataset of naturalistic vehicle trajectories on German highways for validation of highly automated driving systems. In: 2018 21st International Conference on Intelligent Transportation Systems (ITSC), pp. 2118–2125.
Ma, W., Zhong, H., Wang, L., Jiang, L., Abdel-Aty, M., 2022. MAGIC dataset: multiple conditions unmanned aerial vehicle group-based high-fidelity comprehensive vehicle trajectory dataset. Transport. Res. Rec. 2676, 793–805.
Mahmud, S.M.S., Ferreira, L., Hoque, M.S., Tavassoli, A., 2017. Application of proximal surrogate indicators for safety evaluation: a review of recent developments and research needs. IATSS Res. 41, 153–163.
Masouleh, M.K., Shah-Hosseini, R., 2019. Development and evaluation of a deep learning model for real-time ground vehicle semantic segmentation from UAV-based thermal infrared imagery. ISPRS J. Photogrammetry Remote Sens. 155, 172–186.
Messelodi, S., Modena, C.M., 2005. A computer vision system for traffic accident risk measurement. A case study. Adv. Transport. Stud. 7, 51–66.
Mobilithek, 2022. Querschnittsdaten (Q und v) von Messstellen auf BAB in Nordrhein-Westfalen. https://mobilithek.info/offers/110000000003477001.
Moers, T., Vater, L., Krajewski, R., Bock, J., Zlocki, A., Eckstein, L., 2022. The exiD dataset: a real-world trajectory dataset of highly interactive highway scenarios in Germany. In: 2022 IEEE Intelligent Vehicles Symposium (IV), pp. 958–964.
Munkres, J., 1957. Algorithms for the assignment and transportation problems. J. Soc. Ind. Appl. Math. 5, 32–38.
Ozbay, K., Yang, H., Bartin, B., Mudigonda, S., 2008. Derivation and validation of new simulation-based surrogate safety measure. Transport. Res. Rec. 2083, 105–113.
Roesener, C., Sauerbier, J., Zlocki, A., Fahrenkrog, F., Wang, L., Varhelyi, A., et al., 2017. A comprehensive evaluation approach for highly automated driving. In: 25th International Technical Conference on the Enhanced Safety of Vehicles (ESV), Detroit, 0259.
Shi, J., Tomasi, 1994. Good features to track. In: 1994 Proceedings of IEEE Conference on Computer Vision and Pattern Recognition, pp. 593–600.
Shi, X., Zhao, D., Yao, H., Li, X., Hale, D.K., Ghiasi, A., 2021. Video-based trajectory extraction with deep learning for High-Granularity Highway Simulation (HIGH-SIM). Commun. Transport. Res. 1, 100014.
Spannaus, P., Zechel, P., Lenz, K., 2021. Automatum data: drone-based highway dataset for the development and validation of automated driving software for research and commercial applications. In: 2021 IEEE Intelligent Vehicles Symposium, vol. IV, pp. 1372–1377.
Staacks, S., Hütz, S., Heinke, H., Stampfer, C., 2018. Advanced tools for smartphone-based experiments: phyphox. Phys. Educ. 53, 045009.
Treiber, M., Helbing, D., 2002. Reconstructing the spatio-temporal traffic dynamics from stationary detector data. Cooper@tive Tr@nsport@tion Dyn@mics 1, 1–3.
Treiterer, J., 1975. Investigation of traffic dynamics by aerial photogrammetry techniques. Transport. Res. Rec. 224.
U.S. Federal Highway Administration (FHWA), 2006. Next generation simulation program (NGSIM). http://ops.fhwa.dot.gov/trafficanalysistools/ngsim.htm.
Wang, J., Fu, T., Xue, J., Li, C., Song, H., Xu, W., et al., 2023. Realtime wide-area vehicle trajectory tracking using millimeter-wave radar sensors and the open TJRD TS dataset. Int. J. Transp. Sci. Technol. 12, 273–290.
Yeom, S., Nam, D.H., 2021. Moving vehicle tracking with a moving drone based on track association. Appl. Sci. 11, 4046.
Zhao, D., Li, X., 2019. Real-world trajectory extraction from aerial videos-A comprehensive and effective solution. In: 2019 IEEE Intelligent Transportation Systems Conference (ITSC), pp. 2854–2859.
Zhao, H., Cui, J., Zha, H., Katabira, K., Shao, X., Shibasaki, R., 2009. Sensing an intersection using a network of laser scanners and video cameras. IEEE Intell. Transport. Syst. Mag. 1, 31–37.

Moritz Berghaus received the M.Sc. degree in transportation engineering from RWTH Aachen University in 2017, where he is currently pursuing the Ph.D. degree. Since 2018, he has been a Research Assistant with the Institute of Highway Engineering, RWTH Aachen University. His research interests include traffic safety, traffic flow, and simulation.

Serge Lamberty received the M.Sc. degree in electrical engineering, information technology, and computer engineering from RWTH Aachen University in 2017. From 2017 to 2022, he was a Researcher in the field of traffic digitalization and since 2022, he has been heading the Digitization Division at the Institute of Highway Engineering, RWTH Aachen University. His research interests include computer vision in traffic surveillance, real-time traffic data acquisition and analysis, and adaptive warning systems.

Jörg Ehlers received the M.Sc. degree in transportation engineering from RWTH Aachen University. He currently works as a Research Assistant with the Institute of Highway Engineering, RWTH Aachen University. His research interests include traffic safety and transportation systems.

Eszter Kalló received the M.Sc. degree in civil engineering from Budapest University of Technology and Economics in 2017. Since 2018, she has been a Research Assistant with the Institute of Highway Engineering, RWTH Aachen University, where she is currently pursuing the Ph.D. degree. Her research interests include traffic safety, traffic flow, and microscopic traffic data.

Markus Oeser received the Ph.D. degree in civil engineering from TU Dresden in 1998 and 2004, respectively. He was a university Lecturer at the Institute of Geotechnics, Road Construction and Traffic Engineering, University of New South Wales (UNSW), Sydney, from 2007 to 2011. He is currently a Professor with the Institute of Highway Engineering, RWTH Aachen University. From 2015 to 2021, he was Dean of the Faculty of Civil Engineering, RWTH Aachen University. Since 2021, he has been the President of the German Federal Highway Research Institute (BASt). His research interests include pavement and traffic engineering.